Spin, charge, and orbital ordering in Mn perovskite oxides studied by model Hartree-Fock calculations

T. Mizokawa and A. Fujimori

Department of Physics, University of Tokyo, Bunkyo-ku, Tokyo 113, Japan

The spin, charge, and orbital ordering in $R_{0.5}A_{0.5}MnO_3$ and $R_{0.5}A_{1.5}MnO_4$ (R=rare earth, A=Sr, Ca) has been studied by means of unrestricted Hartree-Fock calculations on the multiband p-d model. Since the superexchange interaction between the Mn^{3+} and Mn^{4+} sites depends on which type of e_g orbital is occupied at the Mn^{3+} site, antiferromagnetic states such as A type and CE type favor a specific orbital ordering. It is shown that the Jahn-Teller distortion consistent with the orbital ordering plays an essential role in stabilizing the experimentally observed antiferromagnetic states. [S0163-1829(97)50130-5]

Ferromagnetism and charge ordering in the doped perovskite-type manganese oxides $R_{1-x}A_xMnO_3$ (R=rare earth, A=Sr, Ca) have attracted revived interest since the rediscovery of colossal magnetoresistance.[1] Extensive studies of the manganese oxides as a function of the size of the R and A ions revealed that the $GdFeO_3$-type distortion, which becomes larger as the size of the R and A ions become smaller, stabilizes the charge-ordered (CO) state compared with the ferromagnetic (FM) state. The least distorted $La_{0.5}Sr_{0.5}MnO_3$ is a FM metal below the Curie temperature (T_C) and a paramagnetic insulator above T_C without charge ordering.[2] More distorted $Pr_{0.5}Ca_{0.5}MnO_3$ ($T_{CO}\sim230$ K) (Refs. 3 and 4) and $Nd_{0.5}Ca_{0.5}MnO_3$ ($T_{CO}\sim220$ K) (Ref. 5) become CO insulators below the charge-ordering temperature (T_{CO}) and do not show ferromagnetism. $La_{0.5}Ca_{0.5}MnO_3$ ($T_{CO}\sim160$ K) (Refs. 6 and 7) and $Nd_{0.5}Sr_{0.5}MnO_3$ ($T_{CO}\sim150$ K),[8] which are located between the two extremes, undergo a FM metal to CO insulator transition on cooling. Most of the CO states in these compounds have CE-type AFM order which is well explained by the model proposed by Goodenough.[9] In this model, Mn^{3+} and Mn^{4+} are arranged like a checkerboard (see Fig. 1) and the Mn^{3+} sites have a Jahn-Teller (JT) distortion. The charge ordering and the JT distortion in the CE-type AFM state have been observed by x-ray and neutron diffraction measurements.[3,6,7] Very recently, a neutron diffraction study[10] of $Pr_{0.5}Sr_{0.5}MnO_3$ [$T_{CO}\sim130$ K (Ref. 11)] showed that A-type AFM order sets in below T_{CO}.[12] In addition to the three-dimensional perovskites, the AFM CO state has been observed in the layered perovskite $La_{0.5}Sr_{1.5}MnO_4$,[13] which does not have the $GdFeO_3$-type distortion. It is important to study how the stability of the CO states is controlled by the lattice distortion of $GdFeO_3$ and JT type. Especially, an interesting question is how the orbital degrees of freedom of Mn^{3+}, which couples with the JT distortion, affects the FM metallic versus AFM CO insulating behaviors.

Interplay between the magnetic ordering and the JT distortion has been studied in $RMn^{3+}O_3$ by means of model Hartree-Fock (HF)[14] and local-spin-density approximation (LSDA)[15] band-structure calculations. These calculations have shown that, while the system would be a FM metal

without the JT distortion, $RMn^{3+}O_3$ is the A-type AFM state because of the JT distortion. Since the exchange coupling between Mn^{3+} and Mn^{4+} depends on which type of e_g orbital is occupied at the Mn^{3+} site, there is an interesting interplay between the spin and orbital ordering also in the doped $RMn^{3+}O_3$. In this paper, HF calculations for $R_{0.5}A_{0.5}MnO_3$ and $R_{0.5}A_{1.5}MnO_4$ are presented. The HF cal-
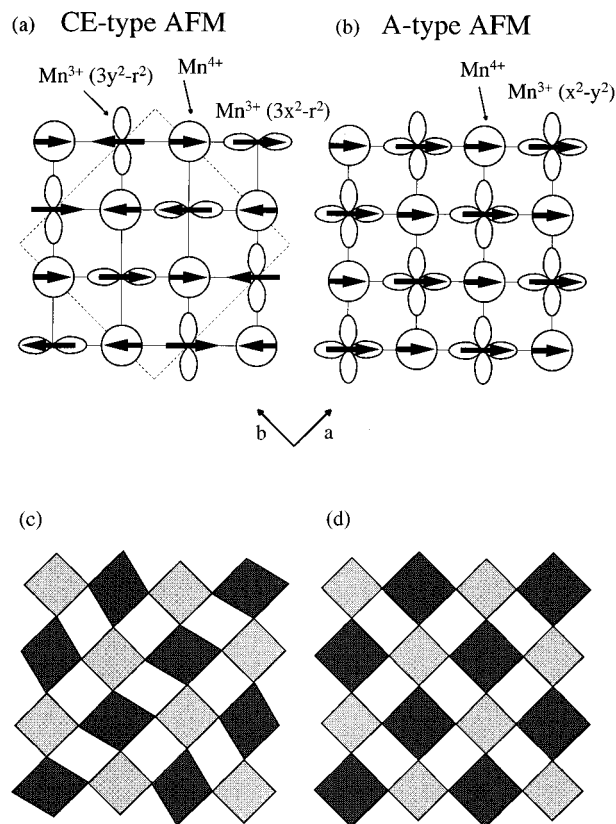

FIG. 1. Upper panel: Spin, charge, and orbital ordering for the CE-type AFM CO state (a) and for the A-type AFM CO state (b). The broken line shows the unit cell for the CE-type AFM CO order. Lower panel: JT distortions consistent with the CE-type AFM CO state (c) and the A-type AFM CO state (d). The dark and light shaded squares show the Mn^{+3} and Mn^{+4} sites, respectively.

culations tell us which type of charge and orbital ordering is favored under a given spin arrangement. We also study the relative stability of various spin, charge and orbital ordered states as a function of the lattice distortion of $GdFeO_3$ and JT type. Based on the result of the calculations, we discuss which type of orbital ordering and lattice distortion are relevant to stabilize the CO state in the doped manganese oxides.

We have employed the multiband d-p model, where the tenfold degeneracy of the Mn $3d$ orbitals and the sixfold degeneracy of the O $2p$ orbitals are taken into account.[14] The intra-atomic Coulomb interaction is expressed by Kanamori parameters, u, u', j, and j'.[16] The charge-transfer energy Δ is defined by $\epsilon_d^0 - \epsilon_p + nU$, where U ($=u-20/9j$) is the multiplet-averaged $d-d$ Coulomb interaction and $n=3.5$ for $R_{0.5}A_{0.5}MnO_3$ and $R_{0.5}A_{1.5}MnO_4$. The transfer integrals between the Mn $3d$ and O $2p$ orbitals are given in terms of Slater-Koster parameters $(pp\sigma)$, $(pp\pi)$, $(pd\sigma)$, and $(pd\pi)$. Δ, U, and $(pd\sigma)$ for $LaMnO_3$ deduced from photoemission spectroscopy[17] are 4, 5.5, and -1.8 eV, respectively. From the Δ and U values, $\epsilon_d^0 - \epsilon_p$ for $LaMnO_3$ is evaluated to be -18 eV. We have used these values of $(pd\sigma)$ and $\epsilon_d^0 - \epsilon_p$ as input for the HF calculations. The ratio $(pd\sigma)/(pd\pi)$ is fixed at -2.16 and $(pp\sigma)$ and $(pp\pi)$ at -0.60 and 0.15 eV, respectively.[18] The unit cells for $R_{0.5}A_{0.5}MnO_3$ and $R_{0.5}A_{1.5}MnO_4$ include 16 and 8 Mn sites, respectively. We have iterated the self-consistency cycle until successive differences of all the order parameters converged to less that 1×10^{-4} by sampling 64 k points in the first Brillouin zone.

Firstly, we have performed the unrestricted HF calculation for the MnO_3 perovskite-type lattice with 180° Mn-O-Mn bond angle to study the spin, charge, and orbital ordering in $R_{0.5}A_{0.5}MnO_3$. Without the JT distortion, the FM state is the lowest in energy and the A type AFM state is the second lowest [see Fig. 2(a)]. The FM and A-type AFM states are metallic and are not accompanied by charge ordering. The CE-type AFM CO solution with a band gap of ~0.6 eV is obtained but is higher in energy than the FM and A-type AFM state. In the CE-type AFM CO state, the Mn^{3+} and Mn^{4+} are interlaced like a checkerboard within the c plane as shown in Fig. 1(a). Along the c axis, the same in-plane arrangement of Mn^{3+} and Mn^{4+} is stacked and the neighboring planes are antiferromagnetically coupled. The Mn^{3+} sites are accompanied by the $3x^2-r^2/3y^2-r^2$-type orbital ordering even without the JT distortion. This is because the e_g orbital of the Mn^{3+} site tends to point the neighboring Mn^{4+} site in order to gain the kinetic exchange energy. The CE-type AFM CO state with the orbital ordering has originally been proposed by Goodenough[9] and has recently been obtained in an LDA+U calculation[19] although its stability relative to the FM and other AFM CO states has not been studied. It is interesting to note that the orbital ordering in $R_{0.5}A_{0.5}MnO_3$ is contrasted with that in $RMnO_3$, which is a mixture of the z^2-x^2/z^2-y^2 type and the $3x^2-r^2/3y^2-r^2$ type when the JT distortion is absent.[14] The calculated magnetic moments at the Mn^{3+} and Mn^{4+} sites are 3.79 and 3.65μ_B, respectively, and the net numbers of $3d$ electrons at the Mn^{3+} and Mn^{4+} sites are 4.45 and 4.36, respectively. Since $RMnO_3$ is
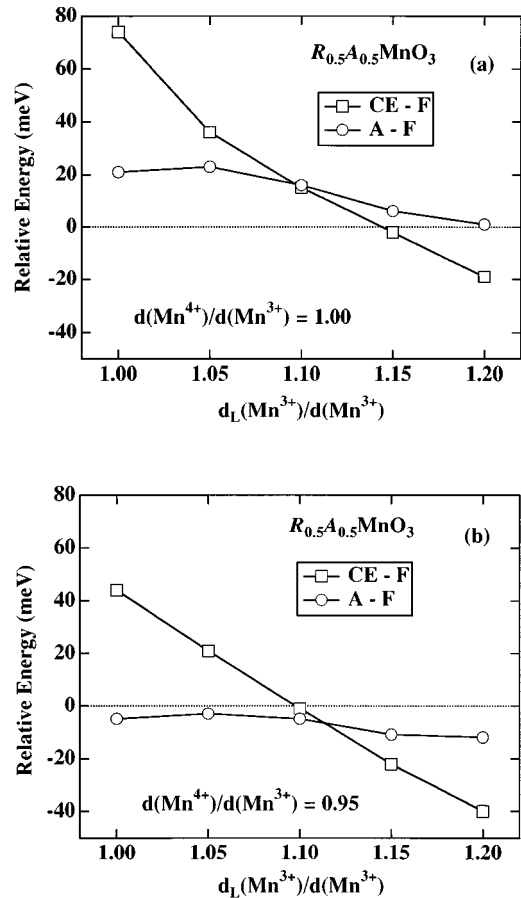

FIG. 2. Energies per formula unit of the CE-type and A-type AFM states relative to the FM state as functions of the JT distortion for the MnO_3 perovskite-type lattice without the in-plane breathing-type distortion (a) and with it (b).

a charge-transfer-type insulator, the net number of $3d$ electrons at the Mn^{4+} sites is close to that at the Mn^{3+} sites. In the present calculation, the C-type and G-type AFM CO states, in which charge and orbital ordering is different from that of the CE-type AFM CO state, are higher in energy than the CE-type AFM CO state.

In Fig. 2(a), we have plotted the energies of the A-type and CE-type AFM states relative to the FM state as functions of the JT distortion that is consistent with the $3x^2-r^2/3y^2-r^2$-type orbital arrangement [Fig. 1(c)]. Although the JT distortion causes a slight tilting of the MnO_6 octahedra, in this model, we have neglected the tilting and included only the JT distortion for simplicity. Here, $d(Mn^{3+})$ and $d(Mn^{4+})$ denote averaged Mn-O bond distances within the c plane around the Mn^{3+} and Mn^{4+} sites, respectively. $d_L(Mn^{3+})$ and $d_S(Mn^{3+})$ are the shorter and longer Mn-O bond distances within the c plane around the Mn^{3+} site, respectively, satisfying the relationship $2d(Mn^{3+})=d_L(Mn^{3+})+d_S(Mn^{3+})$. The Mn-O bond distance along the c axis is kept constant. The transfer integrals are scaled using Harrison's $d^{-3.5}$ law.[18] The present calculation shows that the CE-type AFM state is stabilized by the JT distortion. For $d_L(Mn^{3+})/d(Mn^{3+})=1.15$, the calculated magnetic moments at the Mn^{3+} and Mn^{4+} sites are 3.85 and 3.45μ_B, respectively, and the net numbers of $3d$ electrons at the Mn^{3+} and Mn^{4+} sites are 4.57 and 4.28, respectively.
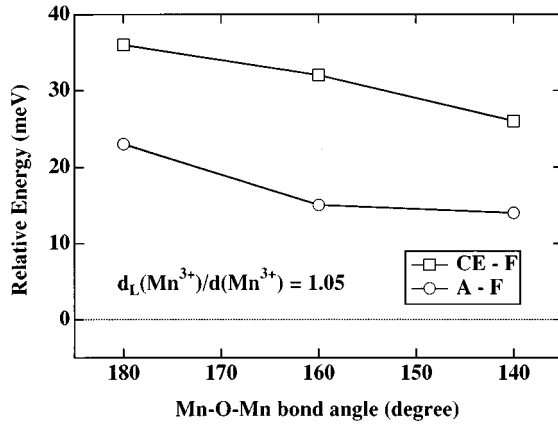
FIG. 3. Energies per formula unit of the CE-type and A-type AFM states relative to the FM state as functions of the Mn-O-Mn bond angle for the MnO_3 perovskite-type lattice.

FIG. 4. Energy per formula unit of the CE-type AFM state relative to the FM state as a function of the JT distortion for the MnO_4 layered perovskite-type lattice.

The difference increases with the JT distortion.

In the A-type AFM CO state, the orbital ordering as shown in Fig. 1(b) is expected to be favored. The orbital order couples with the in-plane breathing-type lattice distortion in which the Mn^{3+} ion is expanded and the Mn^{4+} ion is contracted within the ab plane keeping the Mn-O bond distance along the c axis the same. This breathing-type distortion makes the MnO_6 octahedra at the Mn^{3+} sites expanded with the ab plane and favors the orbital ordering in which the $x^2 - y^2$-type orbital is occupied at the Mn^{3+} sites. We have calculated the energies of the A-type and CE-type AFM states relative to the FM state with the in-plane breathing-type lattice distortion. The relative energies as functions of the JT distortion are shown in Fig. 2(b). Here, $d(Mn^{4+})/d(Mn^{3+})$ is fixed at 0.95. Without the JT distortion, the A-type AFM CO state with the $x^2 - y^2$-type orbital ordering is the lowest in energy and has a band gap of ~ 0.35 eV. The magnetic moments at the Mn^{3+} and Mn^{4+} sites are calculated to be 3.87 and $3.37 \mu_B$, respectively, and the net numbers of $3d$ electrons at the Mn^{3+} and Mn^{4+} sites are 4.51 and 4.36, respectively. This state would be related to the A-type AFM state found in $Pr_{0.5}Sr_{0.5}MnO_3$. However, the difference in the magnetic moment between the Mn^{3+} and Mn^{4+} sites is not observed in $Pr_{0.5}Sr_{0.5}MnO_3$.[10] Under the breathing-type lattice distortion, the JT distortion consistent with the $3x^2 - r^2/3y^2 - r^2$-type orbital ordering also makes the CE-type AFM state the lowest in energy.

We have also calculated the energies of the A-type and CE-type AFM states relative to the FM state in the presence of the $GdFeO_3$-type distortion, namely, as functions of the tilting of the MnO_6 octaherda or the Mn-O-Mn bond angle. The result is shown in Fig. 3. Here, the magnitude of the JT distortion or $d_L(Mn^{3+})/d(Mn^{3+})$ is fixed at 1.05. The tilting of the MnO_6 octaherda does not reduce the energy difference between the AFM states and the FM state very much. The present calculations thus indicate that what is essential to stabilize the CE-type AFM CO state is the JT distortion and not the reduction of the Mn-O-Mn bond angle. Although there is no systematic structural study to reveal the relationship between the $GdFeO_3$-type and JT-type distortions, it is reasonable to assume that the $GdFeO_3$-type distortion causes not only the reduction of the Mn-O-Mn bond angle but also the development of the JT distortion in $R_{0.5}A_{0.5}MnO_3$. The

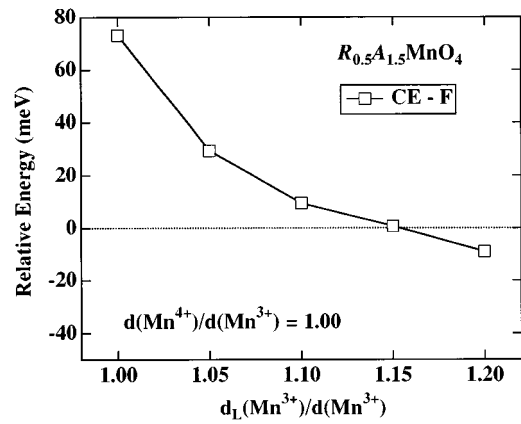present result gives us a scenario that, as the R and A ions become smaller, the magnitude of the JT distortion becomes larger and consequently the JT distortion stabilizes the CE-type AFM CO state.

We have also performed the model HF calculation using the MnO_4 layered perovskite-type lattice in order to study the charge ordering in $R_{0.5}A_{1.5}MnO_4$. In Fig. 4, we have plotted the energy of the CE-type AFM CO state relative to the FM state as a function of the JT distortion. Without the JT distortion, the FM state is lower in energy than the CE-type AFM state which has the $3x^2 - r^2/3y^2 - r^2$-type orbital ordering as shown in Fig. 1(a). In $R_{0.5}A_{1.5}MnO_4$, too, the JT distortion makes the CE-type AFM CO state lower in energy than the FM state.

In conclusion, we have performed the model HF calculations for $R_{0.5}A_{0.5}MnO_3$ and $R_{0.5}A_{1.5}MnO_4$. Without the lattice distortion, the FM metallic state is the lowest in energy. The CE-type AFM state with orbital ordering of the $3x^2 - r^2/3y^2 - r^2$-type is much higher in energy than the FM state. In $R_{0.5}A_{0.5}MnO_3$, the breathing-type distortion stabilizes the A-type AFM state compared with the FM state. On the other hand, both in $R_{0.5}A_{0.5}MnO_3$ and $R_{0.5}A_{1.5}MnO_4$, the JT distortion at the Mn^{3+} site, which is consistent with the $3x^2 - r^2/3y^2 - r^2$-type orbital ordering, favors the CE-type AFM CO state compared with the FM and A-type AFM states. The present calculations show that the JT-type and breathing-type distortions control the relative stability of the various AFM CO states and the FM state and that the $GdFeO_3$ distortion has relatively weak influence on the charge ordering. It would be useful to apply the present method to other $3d$ transition-metal oxides such as nickelates and cobaltites as well as manganites of other hole concentration in order to systematically study the interplay between the spin, charge, and orbital ordering in the doped $3d$ transition-metal oxides.

[1] For early work, see R. M. Kusters, J. Singleton, D. A. Keen, R. McGreevey, and W. Hayes, Physica B **155**, 362 (1989); S. Jin T. H. Tiefel, M. McCormack, R. A. Fastnacht, R. Ramesh, and L. H. Chen, Science **264**, 413 (1994).

[2] A. Urushibara, Y. Moritomo, T. Arima, A. Asamitsu, G. Kido, and Y. Tokura, Phys. Rev. B **51**, 14 103 (1995).

[3] Z. Jirak, S. Krupicka, Z. Simsa, M. Dlouha, and S. Vratislav, J. Magn. Magn. Mater. **53**, 153 (1985).

[4] Y. Tomioka, A. Asamitsu, Y. Moritomo, H. Kuwahara, and Y. Tokura, Phys. Rev. Lett. **74**, 5108 (1995).

[5] T. Vogt, A. K. Cheetham, R. Mahendira, A. K. Raychaudhuri, R. Mahesh, and C. N. R. Rao, Phys. Rev. B **54**, 15 303 (1996).

[6] P. G. Radaelli, D. E. Cox, M. Marezio, S-W. Cheong, P. E. Schiffer, and A. P. Ramirez, Phys. Rev. Lett. **75**, 4488 (1995); P. G. Radaelli, D. E. Cox, M. Marezio, S-W. Cheong, Phys. Rev. B **55**, 3015 (1997).

[7] C. H. Chen and S.-W. Cheong, Phys. Rev. Lett. **76**, 4042 (1996).

[8] Y. Tomioka, A. Asamitsu, Y. Moritomo, H. Kuwahara, and Y. Tokura, Phys. Rev. Lett. **74**, 5108 (1995).

[9] J. B. Goodenough, Phys. Rev. **100**, 564 (1955).

[10] H. Kawano, R. Kajimoto, H. Yoshizawa, Y. Tomioka, H. Kuwahara, and Y. Tokura, Phys. Rev. Lett. **78**, 4253 (1997).

[11] Y. Tomioka, A. Asamitsu, Y. Moritomo, H. Kuwahara, and Y. Tokura, Phys. Rev. Lett. **74**, 5108 (1995).

[12] Although the transition temperature is referred to as the charge-ordering temperature in the work by Tomioka *et al.* (Ref. 11) the neutron diffraction study (Ref. 10) has failed to observed a clear sign of charge ordering.

[13] B. J. Sternlieb, J. P. Hill, U. C. Wildgruber, G. M. Luke, B. Nachumi, Y. Moritomo, and Y. Tokura, Phys. Rev. Lett. **76**, 2169 (1996); Y. Murakami *et al.* (unpublished).

[14] T. Mizokawa and A. Fujimori, Phys. Rev. B **51**, 12 880 (1995).

[15] I. V. Solovyev, N. Hamada, and K. Terakura, Phys. Rev. Lett. **76**, 4825 (1996).

[16] J. Kanamori, Prog. Theor. Phys. **30**, 275 (1963).

[17] A. Chainani, M. Mathew, and D. D. Sarma, Phys. Rev. B **47**, 15 397 (1993); T. Saitoh, A. E. Bocquet, T. Mizokawa, H. Namatame, A. Fujimori, M. Abbate, Y. Takeda, and M. Takano, *ibid.* **51**, 13 942 (1995).

[18] W. A. Harrison, *Electronic Structure and the Properties of Solids* (Dover, New York, 1989).

[19] V. I. Anisimov, I. S. Elfimov, M. A. Korotin, and K. Terakura, Phys. Rev. B (to be published).